Effect of trace potassium on hydrogen adsorption and dissociation on hcp cobalt: A density functional theory study

Qingjun Chen, [a] *Ingeborg-Helene Svenum,* [b] *Ljubisa Gavrilovic,* [a] *De Chen,* [a] *and Edd A. Blekkan* [a,*]

[a] Department of Chemical Engineering, Norwegian University of Science and Technology (NTNU), 7491 Trondheim, Norway.

[b] SINTEF Materials and Chemistry, 7465 Trondheim, Norway

* Corresponding author, Email: edd.a.blekkan@ntnu.no

Abstract:

Trace amounts of potassium (K) have a significant influence on the activity and selectivity of cobalt-based catalysts in Fischer–Tropsch synthesis (FTS), in which hydrogen adsorption and dissociation is one of the initial and most important steps. In this work, hydrogen adsorption and dissociation behavior on typical facets ((0001), (10-11), (10-12), (10-15) and (11-20)) of hcp Co with and without adsorbed K were systematically studied. H_2 molecular adsorption results showed that H_2 mainly adsorbed in the perpendicular mode and close to the state of free H_2. Different facets and pre-adsorbed K did not show obvious effects on the H_2 adsorption energy. Atomic hydrogen adsorption was site and facet dependent, but the maximum hydrogen adsorption energy on the different facets of hcp Co were similar (-2.64 to -2.67 eV) with the exception on the (11-20) facet where the adsorption energy was significantly lower (-2.44 eV). K had a slight

destabilizing effect on the H atom adsorption on the former Co surfaces due to a very weak repulsive interaction between K and H atoms. The initial H_2 dissociation had negligible energy barriers (0-0.07 eV) on the clean surface of hcp Co, suggesting the direct dissociative adsorption of H_2. The energy barriers for H_2 dissociation are mainly caused by the approach of molecular H_2 towards the Co surface and the rotation of the H_2 molecule from the perpendicular mode to the parallel mode. The H_2 dissociation energy barriers increase by 0.02-0.17 eV after the pre-adsorption of K, indicating a slight inhibition of H_2 dissociation by K. However, the energy barriers for H_2 dissociation in the presence of K were also small (0.05-0.21 eV). This indicates that H_2 dissociates readily at typical Co-based FTS reaction temperatures (210-240 ^oC), both in the absence and presence of K. Different K species (K and KOH) exhibit similar effects on H_2 dissociation on hcp Co. The B_5 sites on the stepped facets, the preferred sites for K adsorption are not the most favorable site for H_2 dissociation, and K slightly hinders H_2 dissociation at the B_5 site of hcp Co.

Introduction

Fischer–Tropsch synthesis (FTS), which converts syngas (a mixture of CO and H_2) into valuable chemicals and fuels, is the heart of the gas to liquids (GTL), coal to liquids (CTL) and biomass to liquids (BTL) processes [1-4]. The catalysts for FTS are based on Fe, Co or Ru. Co-based catalysts are selected for natural gas-based processes due to the high activity (per weight), high selectivity to long-chain hydrocarbons, low selectivity to CO_2, as well as high stability and medium price level [1,5-7]. One of the drawbacks regarding Co-based FTS catalysts, is the sensitivity toward impurities such as K, Na, Mg, Ca in the syngas mixture, issues especially important for biomass-derived syngas, the only practical renewable source of carbon [8-10].

Extensive work indicate that trace amounts of alkali metals (from tens to thousands ppm) result in significant decrease of the FTS activity and increase of olefin and C_{5+} selectivities [8,11-13].

FTS is comprised of a complex network of elementary bond-breaking and bond forming steps. These steps include H_2 and CO activation as well as hydrogenation and chain growth over supported metal catalysts [1, 14,15]. The adsorption and dissociation of hydrogen is one of the initial steps in the mechanism and thought to be critical in controlling catalytic activity and selectivity, especially in the H-assisted CO dissociation routes on Co catalysts [1,14-18]. It seems that except for the possible blocking of the most active sites of Co, the presence of K might also affect the H adsorption and thus alter the selectivity of products. Therefore, the study of hydrogen adsorption and dissociation on Co with or without K is of high significance to elucidate the role of K in Co-based FTS.

Experimental investigations showed that trace alkali metal loading (less than 1000 ppm) did not change the heat of adsorption nor the amount of adsorbed hydrogen on Co-based FTS catalysts [8,11-13]. The explanation may be that the trace amount of K itself did not have an effect on hydrogen dissociation and chemisorption on Co surface or that the experimental equipment cannot detect the difference of hydrogen chemisorption due to the sensitivity limitation at very low K concentrations. Theoretical calculations, especially density functional theory (DFT) calculations, can help elucidate the effect of trace amount of K on the hydrogen dissociation and adsorption on hcp Co.

Extensive DFT calculations on hydrogen adsorption and activation have been done on Pd, Pt, Rh, Ni, Cu, Mg, Co, and other metals [19-28]. In general, these results confirm the dissociative adsorption of H_2 on the metal surface. For example, Ferrin et al. studied the adsorption and diffusion of hydrogen on different facets of 17 transition metals, including hcp Co [22]. The results

showed that the formation of surface hydrogen is exothermic with respect to gas-phase H_2 on all metals with the exception of Ag and Au. Wang et al. discussed the adsorption and activation of hydrogen on different facets of Co and concluded that dissociative adsorption dominates independent of coverage and surface structure [23]. On the other hand, van Helden et al. revealed that hydrogen adsorption was coverage dependent and that steps and defects will expose a broad range of adsorption sites with varying (mostly less favorable) adsorption energies [24]. In addition, pre-covered species such as S, K, C, CO, and even transition metals affected the dissociation of hydrogen. Scheffler et al. calculated the poisoning of Pd for dissociation of H_2 by sulfur and concluded that the poisoning effect of sulfur adatoms for H_2 dissociation at low sulfur coverage (<0.25 ML) was mainly governed by the formation of energy barriers and a modest decrease of the adsorption energy in the vicinity of the sulfur adatoms, not by the blocking of adsorption sites [25,26]. van Steen and van Helden found that the presence of CO and C blocks several sites for hydrogen adsorption as well as increasing the hydrogen dissociation barriers on Fe(100) [27]. Wilke and Cohen investigated the effect of K adatoms on the dissociative adsorption on Pd (100) and found that K induced energy barriers for hydrogen dissociation in the entrance channel, and hindered the approach of the molecules to the surface [28]. The body of work discussed here provides valuable information about H_2 adsorption and dissociation on Co with or without promoters. However, the adsorption and dissociation behavior of hydrogen on typical facets of hcp Co with or without low coverage of K (<0.1 ML) are not clear, features that are important in order to understand the role of trace K in the activity and selectivity of Co-based FTS catalysts.

In our previous work, the K adsorption behavior was systematically studied on the predicted exposed facets of hcp Co particles [29]. The results showed that that K adsorption was favorable on all these facets, with the stepped facet (10-12) exhibiting the largest K adsorption energy. In

this work, we address hydrogen adsorption and dissociation on the terrace (0001), terrace-like ((10-11)), stepped ((10-12) and (10-15)) and corrugated ((11-20)) facets on hcp Co, and the effect of pre-adsorbed K species. K species in the form of K and KOH are discussed.

2. Methods and models

DFT calculations were performed using the Vienna ab initio Simulation Package (VASP) [30-31]. The projector augmented wave (PAW) method was used to describe the interactions between ion cores and valence electrons [32]. The plane wave energy cutoff is set to 500 eV [29]. The exchange correlation energy of the electrons was treated with the GGA-PBE functional [33]. The sampling of the Brillouin zone was performed using a Monkhorst−Pack scheme [34]. Bulk hcp Co has the P63/MMC crystallographic symmetry and contains two Co atoms per unit cell. According to our previous calculation, the equilibrium lattice of the bulk hcp Co are a=b=2.491 Å and c=4.023 Å, which are in good agreement with experimentally determined values of a=b=2.507Å and c=4.069 Å [35]. Here, we use the same bulk hcp Co for the calculation of hydrogen adsorption and dissociation.

In order to study the adsorption and dissociation of H_2 at low coverages of K (around 0.05 ML), slabs with minimum 64 Co atoms distributed in 4 layers separated by a vacuum region of about 15 Å were used. The monolayer (ML) is defined as one K atom per Co surface atom. The coverage of K was defined as the ratio of the number of K atoms to Co atoms in top layer. The top two layers of Co atoms were allowed to relax during optimization, while the bottom two layers were fixed at their corresponding bulk positions. The detailed Monkhorst-Pack k-point sampling for different facets can be seen from our previous work [29].

The adsorption energy of molecular and atomic hydrogen with or without K was defined as $E_{ads} = (E_{adsorbate/surface} - (E_{surface} + E_{adsorbate}))$, where $E_{adsorbate/surface}$ was the total energy of the Co surface (clean or with K/KOH pre-adsorbed) with adsorbates (H_2 or H), $E_{surface}$ was the total energy of the corresponding Co surface (clean or with K/KOH pre-adsorbed), and $E_{adsorbate}$ was the total energy of free adsorbate in the gas phase (H_2 or H). A negative value of E_{ads} represents favorable adsorption. The adsorption of H_2 and H atom were calculated by initially placing the adsorbate above different high symmetry sites of the typical facets of hcp cobalt (as described previously [29]).

H_2 dissociation energy barrier (E_a) and reaction energy (ΔE) are calculated on the basis of the following formulas:

$$E_a = E_{TS} - E_{IS}$$

$$\Delta E = E_{FS} - E_{TS,}$$

Where E_{IS}, E_{FS}, and E_{TS} are the total energies of Co surface (clean or K/KOH re-adsorbed) along with the H_2 molecular, dissociated H atoms, and the transition states. The transition states were investigated using climbing image nudged elastic band method (CI-NEB) [36] and further refined using the Dimer method [37], and finally verified by vibrational analysis yielding a single imaginary frequency. Zero-point energy was included in the adsorption/reaction energies and activation barriers.

3. Results and Discussion

3.1. Adsorption of molecular and atomic hydrogen on clean surfaces of hcp Co

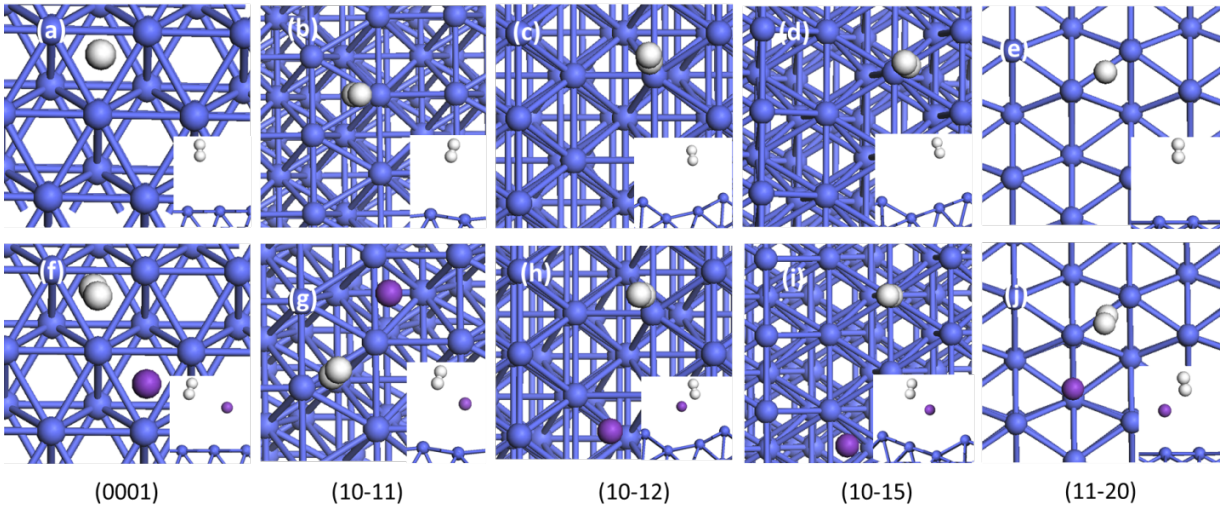

Fig. 1 Stable H_2 adsorption configurations on different facets of hcp Co without (a, b, c, d, e) and with (f, g, h, i, j) pre-adsorbed K. Inserts are in side view. The Co, H and K atoms are shown in blue, white and purple balls, respectively, and similarly hereinafter.

Our previous work predicted that hcp Co particles consist of 10 facets. K adsorption were favored on all these facets, with the stepped facet (10-12) showing the highest K adsorption energy [29]. In this work, H_2 adsorption and dissociation were studied on selected facets of the hcp Co: terrace facet (0001), terrace-like facet (10-11)) stepped facets (10-12) and (10-15) and the corrugated facet (11-20). Adsorption of molecular hydrogen was first calculated on the clean surfaces of hcp Co. There were two orientation modes for H_2 molecular adsorption: parallel and perpendicular (or vertical) modes. Our results indicated that H_2 adsorbed in the parallel mode was not stable. In this case, H_2 dissociated on top of the Co, and the two H atoms were adsorbed separately on different sites on the surface (can be seen below from Fig. 3a, f). This result is in agreement with the work of Wang et al. [23]. In the perpendicular mode, the H_2 molecule could be stably adsorbed on hcp Co with the H-H bond slightly tilted compared to the surface normal.

Thus, the adsorption of H_2 presented here was mainly calculated with hydrogen in the perpendicular mode.

H_2 molecular adsorption results on different facets of hcp Co are presented in Fig. 1 and Table 1. On all investigated facets the adsorption energies of the H_2 molecule are very small (0 to -0.02 eV). The H_2 molecule is located relatively far from the surfaces (> 3.7 Å) as shown in the inserts of Fig. 2 and listed in Table 1. No significant difference is predicted depending on the site or facet orientation. This confirms that the interaction of molecular H_2 with hcp Co is very weak, and the adsorbed states of H_2 are close to the free H_2 molecule.

Atomic hydrogen adsorption depends is site and facet dependent. The favored adsorption site and corresponding energy is listed in Table 1. Taking the (0001) facet as an example, H atom favors hollow sites (fcc and hcp). An H atom initially placed at top or bridge sites transfers to hollow sites. The adsorption of H is slightly more favorable in the fcc hollow (see Fig. 2) with an adsorption energy of -2.64 eV, with H in the hcp hollow 0.05 eV less stable. Also on facets (10-11), (10-12) and (10-15), H prefers the three fold hollow sites as displayed in Fig. 2 with similar adsorption energies around -2.65 eV. The adsorption energies of H atom calculated here have be corrected by the zero-point energy (ZPE). The initial H atom adsorption energies before ZPE correction are about -2.85 eV, corresponding to the literature [22,23]. On the corrugated facet (11-20), the most stable H adsorption site is the bridge site (BG, Fig. 2e). The H adsorption energy of -2.44 eV is considerably lower on this facet compared to that of the other facets. In addition, the nearest distance between H and Co atoms (d_{Co-H}) on this facet is shorter (1.668 Å) than on the other facets (1.728-1.741 Å, Table 1). According to the results in Table 1, with the exception of the corrugated facet, the H adsorption energies are similar on the different facets investigated (-2.64 to -2.67 eV).

Table 1. Energies and structural parameters for H and H_2 adsorption on clean and K-pre-adsorbed Co surfaces.

Facet	Slab (unit cell)	Surface or coverage of K	H adsorption site	$E_{ads\text{-}H}$[a] (eV)	$E_{ads\text{-}H2}$[b] (eV)	$d_{Co\text{-}H}$[c] (Å)	$d_{Co\text{-}H2}$[d] (Å)
(0001)	p(4×4)	Clean	fcc Hollow	-2.64	-0.01	1.740	3.940
		K pre-adsorbed (0.063ML)	fcc Hollow	-2.62	-0.01	1.731	4.011
(10-11)	p(2×4)	Clean	3F Hollow	-2.67	0	1.734	4.000
		K pre-adsorbed (0.063ML)	3F Hollow	-2.65	0	1.739	4.010
(10-12)	p(2×4)	Clean	3F Hollow	-2.67	-0.01	1.728	3.734
		K pre-adsorbed (0.042ML)	3F Hollow	-2.66	0	1.728	3.730
(10-15)	p(1×4)	Clean	3F Hollow	-2.67	-0.02	1.731	3.897
		K pre-adsorbed (0.042ML)	3F Hollow	-2.63	0	1.741	3.875
(11-20)	p(3×3)	Clean	BG	-2.44	-0.01	1.668	3.999
		K pre-adsorbed (0.028ML)	BG	-2.54	-0.02	1.667	3.898

Note, a, adsorption energy of H atom; b, adsorption energy of molecular H_2; c, the nearest distance between H and Co atoms for H atom adsorption; d, the nearest distance between H and Co atoms for H_2 molecular adsorption.

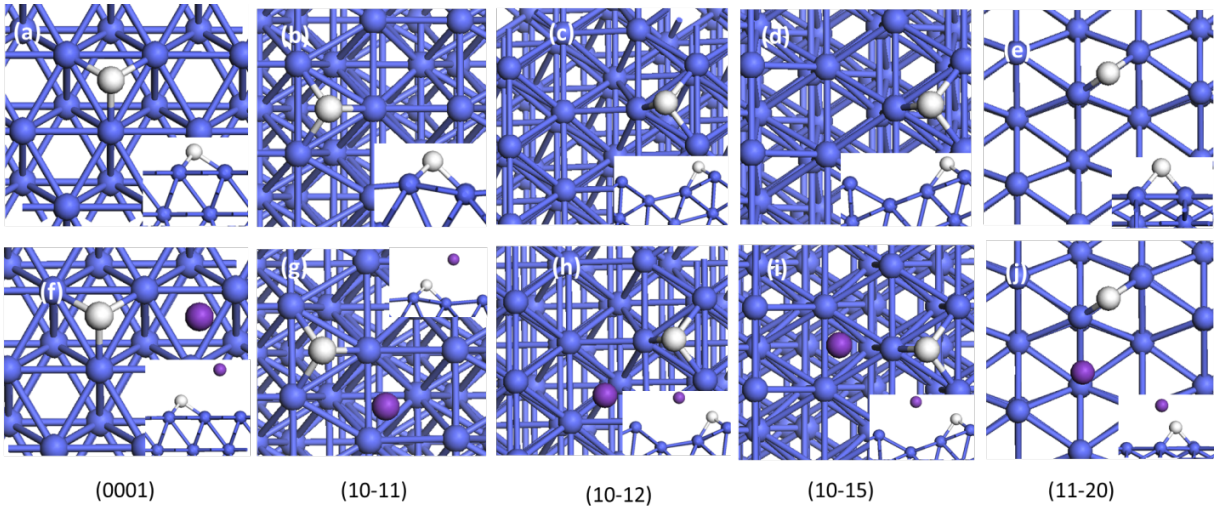

Fig. 2. H atom adsorption configurations on different facets of hcp Co without (a, b, c, d, e) and with (f, g, h, i, j) pre-adsorbed K. Inserts are in side view.

3.2. Effect of K on the adsorption of molecular and atomic hydrogen on hcp Co

As a poison of Co-based FTS catalyst, K might also affect the adsorption of molecular and atomic hydrogen on hcp Co. The results for molecular adsorption of hydrogen on hcp Co with pre-adsorbed K are presented in Table 1 and Fig. 1. As seen from Fig. 1, the stable H_2 adsorption configurations were slightly perturbed by the presence of K on the Co surfaces. At the same time, K was slightly displaced from its original location it occupied without H_2 [29]. These results suggest a very mild repulsive interaction between K and molecular H_2 on these Co facets. However, the H_2 adsorption energy is similar in the presence of K for all the surfaces investigated (Table 1), indicating a very weak H_2 interaction with K. Therefore, K showed negligible effects on the adsorption of molecular hydrogen on hcp Co.

The effect of K on H atom adsorption are shown in Table 1 and Fig. 2. The presence of K leadsto a slight modulation of the H adsorption energy. The adsorption of H was weakened by 0.01-0.04 eV due to K on all the Co facets investigated except (11-20), indicative of a weak repulsive interaction. On these surfaces, the K atom was slightly shifted from its most stable sites

on clean surface and away from H atom as illustrated Fig. 2. In the case of (11-20), adsorption of H was enhanced by 0.10 eV with K pre-adsorbed on the surface. These results suggest that the overall effect of K on H atom adsorption on hcp Co should be a very mild inhibition.

3.3 Hydrogen dissociation on clean surfaces of hcp Co

H_2 dissociation was first calculated on the clean surfaces of hcp Co. The initial state of H_2 dissociation is shown in Fig. 1, and corresponding the transition states (a, b, c, d, e) and final states (f, g, h, i, j) are shown in Fig. 3, respectively. The energies for H_2 dissociation and H-H bonding length in the transition states are presented in Table 2. There are neglectable energy barriers (0-0.02 eV) for H_2 dissociation on (10-11), (10-12), (10-15), and (11-20) facets, suggesting the direct dissociation adsorption of H_2 on these facets. On the terrace facet (0001), the H_2 dissociation barrier is significantly higher, but still very low (0.07 eV). H_2 dissociation on the different facets are all exothermic as shown in Table 2, and the reaction energy is largest at the 3F Hollow site on (10-15) facet. It is interesting to find that the H_2 molecule turns from the perpendicular mode in the initial state (Fig. 1) to the parallel mode (Fig. 3) in the transition states. In the transition state, the H_2 molecule is located just above the Top site of Co atom. Furthermore, the nearest distances between H and Co atoms at the transition states are in the range of 1.575-2.732 Å (Table 2), much smaller than those of the initial states (> 3.7 Å, Table 1). These results indicate that the energy barriers for H_2 dissociation are mainly caused by the approaching of H_2 molecule from far away to the Top site of the Co and the turning of the H_2 molecule from the perpendicular mode to the parallel mode. At the transition states, except on the facet of (10-15), the H-H bond length (0.756~0.759 Å, Table 2) was only slightly stretched compared with the initial state, and thus the energy barriers are not caused by the stretching of the H-H bond. In the case of (10-15) facet, the

H-H bond at the transition state is 1.206 Å, and it seems that the stretching of the H-H bond also contributed to the energy barrier. However, the energy barrier of H_2 dissociation is close to zero on this facet, which further confirms that stretching of the H-H bond has a negligible contribution to the barrier in initial H_2 dissociation on the surface of hcp Co.

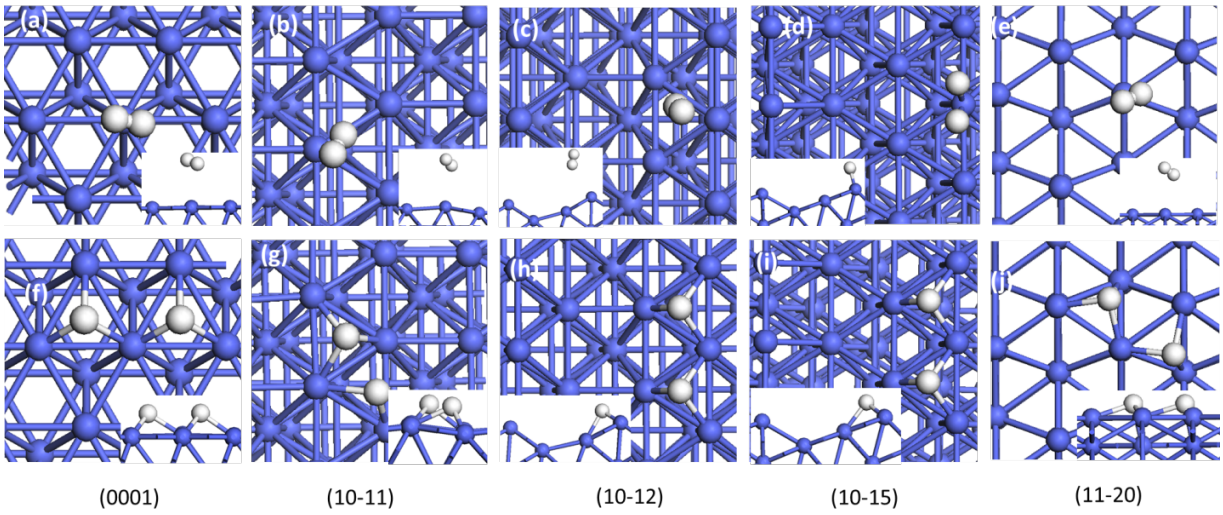

Fig. 3. Illustrations of the transition (a, b, c, d, e) and final states (f, g, h, i, j) for H_2 dissociation on clean surface of hcp Co. Inserts are in side view.

Table 2. H_2 dissociation results on different facet of hcp Co with and without K

Facet	Surface or coverage of K	active site	d_{H-H}[a] (Å)	d_{Co-H}[b] (Å)	E_a (eV)	ΔE (eV)
(0001)	Clean	fcc Hollow	0.759	2.487	0.07	-1.03
	K pre-adsorbed (0.063ML)	fcc Hollow	0.762	2.383	0.14	-0.94
	KOH pre-adsorbed	fcc Hollow	0.768	2.354	0.16	-0.92
(10-11)	Clean	3F Hollow	0.757	2.569	0.01	-0.78
	K pre-adsorbed (0.063ML)	3F Hollow	0.754	2.434	0.07	-0.74
(10-12)	Clean	3F Hollow	0.756	2.732	0.02	-0.59
	K pre-adsorbed (0.042ML)	3F Hollow	0.765	2.312	0.05	-0.55
	Clean	B_5 site[c]	0.765	2.399	0.15	-0.65
	K pre-adsorbed (0.042ML)	B_5 site	0.769	2.318	0.21	-0.62
(10-15)	Clean	3F Hollow	1.206	1.517	0	-1.04
	K pre-adsorbed (0.042ML)	3F Hollow	0.758	2.514	0.02	-1.02
	Clean	B_5 site	1.182	1.520	0.05	-0.98
	K pre-adsorbed (0.042ML)	B_5 site	0.764	2.388	0.15	-0.96
(11-20)	Clean	BG	0.769	2.524	0.01	-0.62
	K pre-adsorbed (0.028ML)	BG	0.776	2.174	0.18	-0.57

Note: a, distance between H atoms; b, the nearest distance between H and Co atoms for H adsorption, c, the B_5 site was defined according to the work of van Hardeveld and Hartog and van

Helden and coworkers [38,39]. The "B_5-site" is used throughout to indicate an ensemble of 5 surface atoms on stepped or rippled facets (e.g. (10-11), (10-12) and (10-15)).

3.4. Effect of K on H_2 dissociation on hcp Co

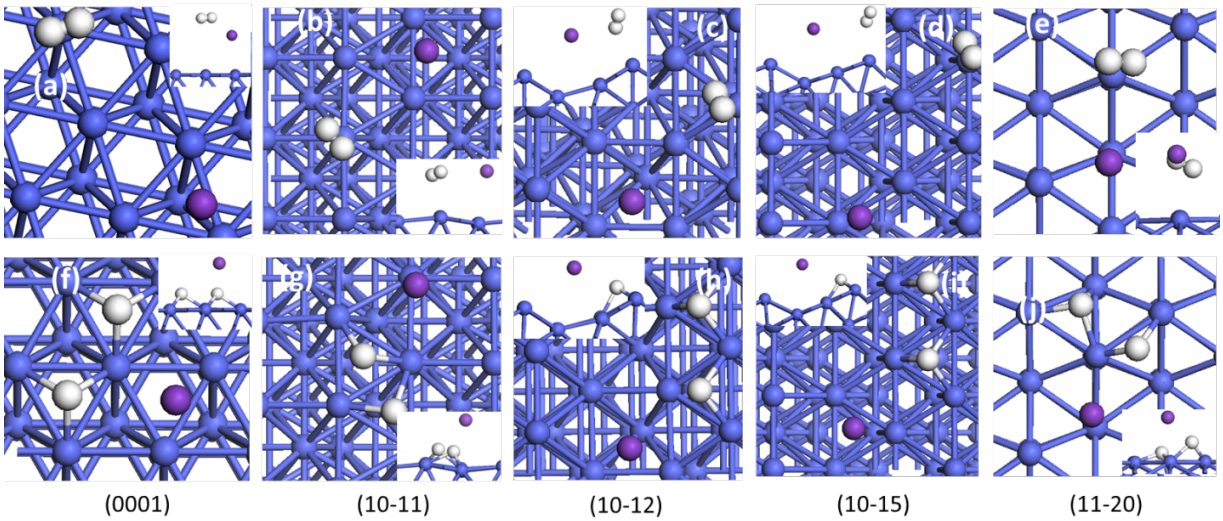

Fig. 4. The transition states (a, b, c, d, e) and final states (g, h, i, j, k) of H_2 dissociation on K pre-adsorbed surface of hcp Co. Inserts are in side view.

The initial states, transition and final states of hydrogen dissociation with low coverages of K (0.028~0.063 ML) are shown in Fig. 2 (f, g, h, i, j) and Fig. 4. The activation energies for H_2 dissociation and H-H bonding length at the transition states in the presence of K are also presented in Table 2. For all facets investigated, the H_2 dissociation energy barriers increased by 0.02-0.17 eV after the pre-adsorption of K, indicating a slight inhibition of H_2 dissociation by K. However, the energy barriers for H_2 dissociation in the presence of K were relatively small (0.05-0.21 eV), indicating that H_2 dissociates readily at room temperature or typical Co-based FTS reaction temperature (210-240 ^oC) [1,5]. In addition, K has negligible effect on the adsorption of H atoms as shown in Table 1. Therefore, for the coverages of K investigated here (up to 0.063 ML) we see

almost no effect on the H_2 chemisorption on the Co catalysts, in agreement with experimental results [8,11-13]. Although the energy barriers for H_2 dissociation increased in the presence of K and the reaction energies decreased on every facet calculated, the changes were marginal only.

The transition states of hydrogen dissociation on K-precovered surface are similar to those without K, where the molecular H_2 is in the parallel mode and just above the Top site of Co atom (Fig. 4). The differences are that the H-H bond length and the nearest distance between H and Co atoms are shorter than those without K (Table 2). It seems that the H_2 approaches closer to the surface of Co before reaching the transition state of dissociation in the presence of K. Furthermore, it is noted that the distance between K and H_2 molecule in the transition states (Fig. 4) are larger than in the initial and the final states (Fig. 2 and Fig. 4). This indicates that there is a repulsive interaction between H_2 molecule and K atom, which inhibits the dissociation of H_2. These findings are in agreement with the results of Wilke and Cohen who reported that K hindered the approach of the molecule to the surface of Pd and induced energy barriers for hydrogen dissociation [28].

Under typical FTS conditions, K might be adsorbed on the Co surface in the form of K atoms, K_2O, or KOH. Experimental results indicate that K is mainly in the form of elemental K (atomic K) or KOH [40,41]. The presence of K_2O on the catalysts surface is less likely due to the relatively high partial pressure of water typically occurring under traditional FTS condition [40,41]. Here, we have also evaluated the effect of KOH on the dissociation of hydrogen on hcp Co. Taking the terrace facet (0001) as an example, the initial, transition and final states of H_2 dissociation in the presence of KOH are shown in Fig. 5. The H_2 dissociation results on (0001) facet with KOH are also listed in Table 2. The H_2 dissociation energy barriers (0.16 vs 0.14 eV) and reaction energies are similar in the presence of KOH as compared to K pre-adsorbed on the Co (0001) facet. The transition states of H_2 dissociation were also similar (parallel mode and above the Top site of Co

atom) for the two different K species. This indicates that there is no significant difference between the effect of K and KOH on the initial dissociation of hydrogen.

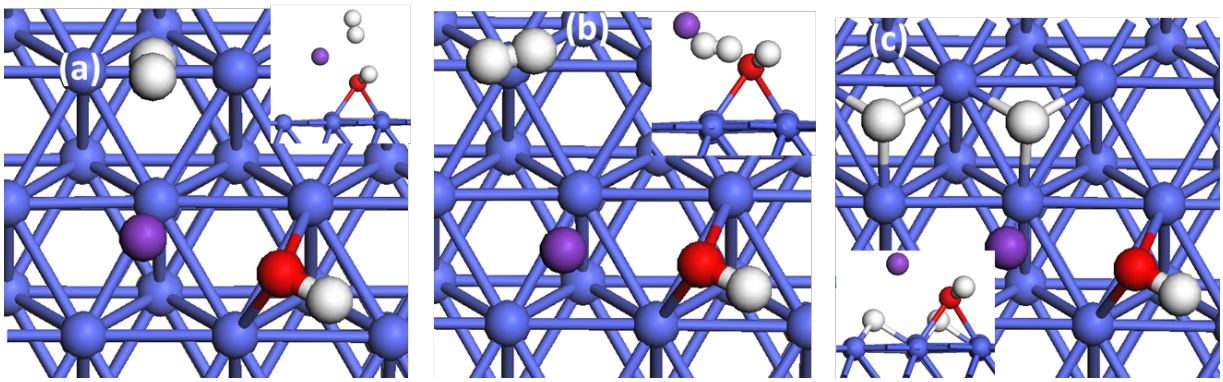

Fig. 5 H_2 dissociation on Co(0001) in the presence of KOH: initial (a), transition state (b) and final state (c), The Co, H, K, and O atoms are shown in the blue, white and purple balls, and red, respectively. Inserts are in side view.

3.5. H_2 dissociation on B_5 sites of hcp Co with and without K

Many studies have suggested that the B_5 sites on the stepped facet of Co might play an important role in the FTS [39,41-43]. Our previous results showed that B_6 site (B_5 site plus a Co atom) on the (10-12) facet exhibited the highest K adsorption energy at low loadings [29], whereas K in the B_5 site on the (10-15) facet was slightly less favorable. Therefore, it is interesting to study the H_2 dissociation at B_5 sites of the stepped facets with and without K. The H_2 dissociation results at B_5 sites of the stepped facets (10-12) and (10-15) with and without K are shown in Fig. 6, Fig. 7 and Table 2. On the clean (10-12) facet, the H_2 dissociation energy barrier at the B_5 site (Fig. 6) is 0.15 eV, distinctly higher than that at the 3-fold (3F) hollow site (0.05 eV). The pre-adsorption

of K on the adjacent B_6 site slightly increased the dissociation barrier [29]. In the transition state, the H atoms are also arranged in a parallel mode with the surface, both in the presence and absence of K.

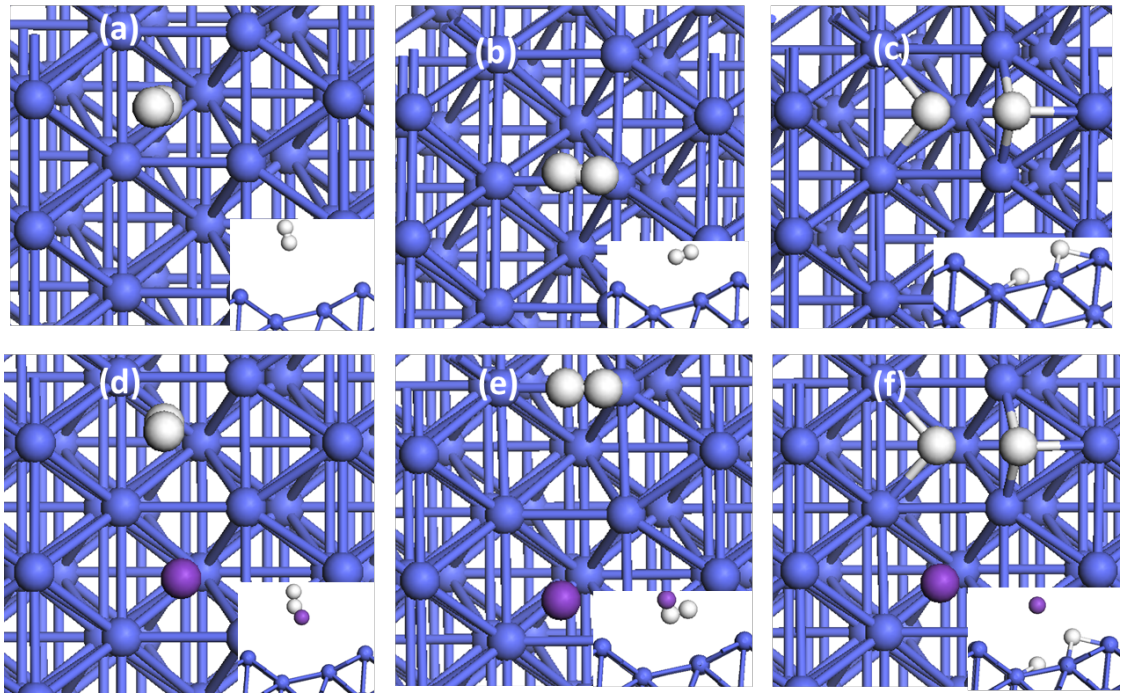

Fig. 6 H_2 dissociation on stepped site (10-12) with (d, e, f) and without K (a, b, c): initial (a,d), transition (b, e) and final states (c, f). Inserts are in side view.

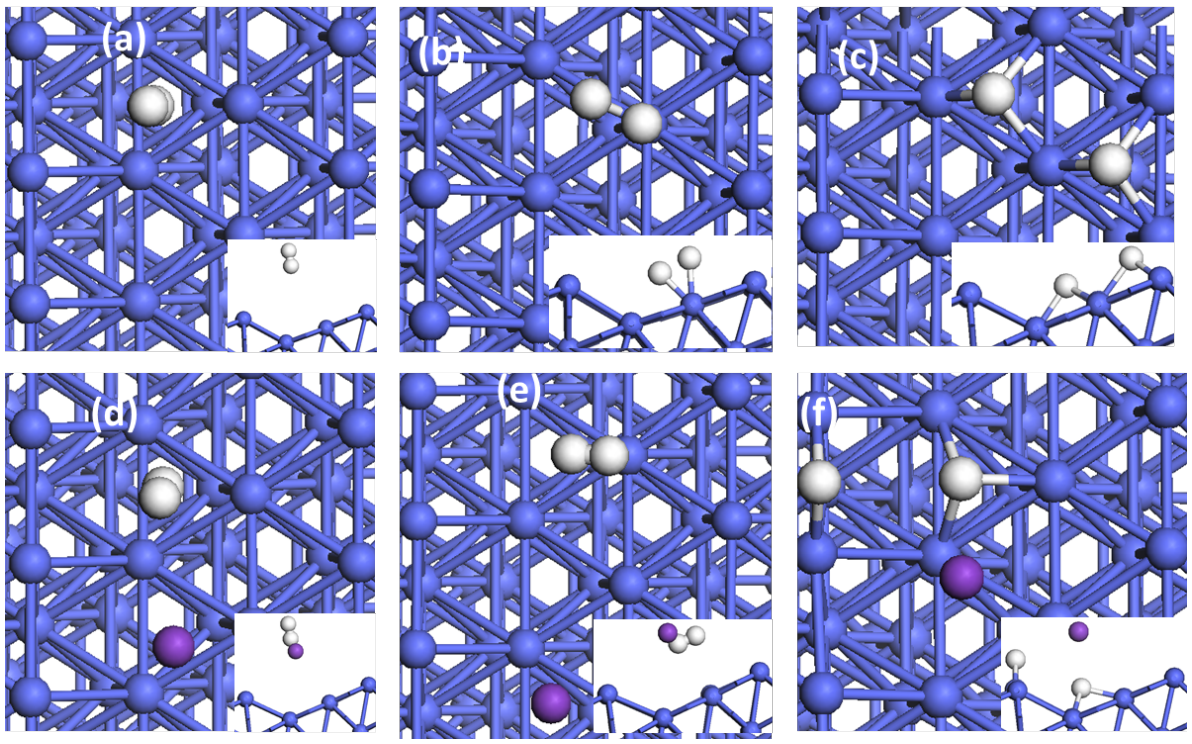

Fig. 7 H_2 dissociation on B_5 site of stepped site (10-15) with (d, e, f) and without K (a, b, c): initial (a,d), transition (b, e) and final states (c, f). Inserts are in side view.

On the clean (10-15) facet, the H_2 dissociation energy at the B_5 site is 0.05 eV, lower compared to the B_5 site on the (10-12) facet, but slightly higher than the more flat facets. At the transition state of H_2 dissociation, the H-H bond length at B_5 site of (10-15) facet (1.520 Å) is similar to that at the 3-fold hollow site (1.517 Å), but significantly different to that at the B_5 site of the (10-12) facet (0.765 Å). When K is pre-adsorbed on the B_6 site of the (10-15) facet, the H_2 dissociation energy barrier increased significantly to 0.15 eV, suggesting an inhibition effect of K for H_2 dissociation. These results indicate that the B_5 sites on the stepped facets are not the most favorable sites for the initial H_2 dissociation and confirm that K slightly hinders H_2 dissociation.

All the results described above showed that H_2 undergoes direct dissociation adsorption on hcp Co with negligible energy barriers (0-0.07 eV). The presence of trace amount of K (0.028-0.063ML) slightly increased the energy barriers (0.05-0.21 eV) for H_2 dissociation, but H_2 still

dissociates readily at typical Co-based FTS reaction temperature due to the very small energy barrier. In addition, K has a slight destabilizing effect on the H atom adsorption (adsorption energy decreased by 0.01~0.04 eV), which is expected to hardly affects the hydrogen chemisorption amounts and adsorption heat as also indicated by the experimental work [8,11-13]. Therefore, the significant decrease of Co-based FTS activity with trace K is not caused by the inhibition of hydrogen dissociation and adsorption by K.

4. Conclusions

Hydrogen adsorption and dissociation on typical facets ((0001), (10-11), (10-12), (10-15), (11-20)) of hcp Co with and without K were systematically studied using density functional theory. H_2 molecular adsorption results showed that H_2 was mainly adsorbed in the form of perpendicular mode and close to the state of free molecular H_2. Different facets and pre-adsorbed K did not show significant effects on the H_2 adsorption energy. Atomic hydrogen adsorption varies depending on site and facet , but the maximum hydrogen adsorption energy on different facets of hcp Co are similar (-2.64 eV vs -2.67 eV). The exception is the (11-20) facet which exhibited a significantly lower adsorption energy compared to the other facets (-2.44 eV). K leads to a slight weakening of the H adsorption energy. H_2 dissociation barriers on the clean surfaces of hcp Co investigated were almost negligible (0-0.07 eV), suggesting the direct dissociation adsorption of H_2. These barriers increased by 0.02-0.17 eV after pre-adsorption of K, indicating a slight inhibition of H_2 dissociation by K. However, the energy barriers for H_2 dissociation in the presence of K still small (0.05-0.21 eV), indicating that H_2 dissociates readily at typical Co-based FTS reaction temperatures (210-240 ^{o}C). Different K species (K and KOH) exhibited similar effect on the dissociation of hydrogen on hcp Co. The results obtained in this work suggest that the significant

decrease observed experimentally in Co-based FTS activity due to trace amount of K is not caused inhibiting activation of H_2.

Acknowledgements

This work has been financially supported by the ENERGIX program in the Norwegian Research Council, project no. 228741. The computations were performed on resources provided by UNINETT Sigma2 - the National Infrastructure for High Performance Computing and Data Storage in Norway, account no. NN9355k and NN9336k.

References

[1] A.Y. Khodakov, W. Chu, P. Fongarland, Advances in the development of novel cobalt Fischer−Tropsch catalysts for synthesis of long-chain hydrocarbons and clean fuels, Chem. Rev., 107 (2007) 1692-1744.

[2] A.P. Steynberg, Chapter 1 - Introduction to Fischer-Tropsch technology, Stud. Surf. Sci. Catal. 152 (2004) 1-63.

[3] E. Jin, Y. Zhang, L. He, H. G. Harris, B. Teng, M. Fan, Indirect coal to liquid technologies, Appl. Catal. A 476 (2014) 158-174.

[4] S. S. Ail, S. Dasappa, Biomass to liquid transportation fuel via Fischer Tropsch synthesis–Technology review and current scenario, Renew. Sust. Energy Rev. 58 **(**2016) 267-286.

[5] B.H. Davis, Fischer-Tropsch synthesis: comparison of performances of iron and cobalt catalysts, Ind. Eng. Chem. Res. 46 (2007) 8938-8945.

[6] Q. Chen, G. Liu, S. Ding, M.C. Sheikh, D. Long, Y. Yoneyama, N. Tsubaki, Design of ultra-active iron-based Fischer-Tropsch synthesis catalysts over spherical mesoporous carbon with developed porosity, Chem. Eng. J. 334 (2018) 714-724.

[7] C. Lian, Y. Yu, K. Zhang, A. Gao, Y. Wang, Highly efficient Fischer–Tropsch synthesis over an alumina-supported ruthenium catalyst, Catal. Sci. Technol. 8 (2018) 1528-1534.

[8] L. Gavrilović, J. Brandin, A. Holmen, H.J. Venvik, R. Myrstad, E.A. Blekkan, Fischer-Tropsch synthesis-Investigation of the deactivation of a Co catalyst by exposure to aerosol particles of potassium salt, Appl. Catal. B 230 (2018) 203-209.

[9] M.K. Gnanamani, V.R.R. Pendyala, G. Jacobs, D.E. Sparks, W.D. Shafer, B.H. Davis, Fischer–Tropsch synthesis: Effect of halides and potassium addition on activity and selectivity of cobalt, Catal. Lett. 144 (2014) 1127-1133.

[10] Ø. Borg, N. Hammer, B.C. Enger, R. Myrstad, O.A. Lindvåg, S. Eri, T.H. Skagseth, E. Rytter, Effect of biomass-derived synthesis gas impurity elements on cobalt Fischer–Tropsch catalyst performance including in situ sulphur and nitrogen addition, J. Catal. 279 (2011) 163-173.

[11] A.H. Lillebø, E. Patanou, J. Yang, E.A. Blekkan, A. Holmen, The effect of alkali and alkaline earth elements on cobalt based Fischer–Tropsch catalysts, Catal. Today 215 (2013) 60-66.

[12] C.M. Balonek, A.H. Lillebø, S. Rane, E. Rytter, L.D. Schmidt, A. Holmen, Effect of alkali metal impurities on Co–Re catalysts for Fischer–Tropsch synthesis from biomass-derived syngas, Catal. Lett. 138 (2010) 8-13.

[13] E. Patanou, A.H. Lillebø, J. Yang, D. Chen, A. Holmen, E.A. Blekkan, Microcalorimetric studies on Co–Re/γ-Al_2O_3 catalysts with Na impurities for Fischer–Tropsch synthesis, Ind. Eng. Chem. Res. 53 (2014) 1787-1793.

[14] C. K. Rofer-DePoorter, A comprehensive mechanism for the Fischer-Tropsch synthesis, Chem. Rev. 81 (1981) 447-474.

[15] G.P. Van Der Laan, A.A.C.M. Beenackers, Kinetics and selectivity of the Fischer–Tropsch Synthesis: A literature review, Catal. Rev. 41 (1999) 255-318.

[16] R. Zhang, F. Liu, Q. Wang, B. Wang, D. Li, Insight into CH_x formation in Fischer–Tropsch synthesis on the hexahedron Co catalyst: Effect of surface structure on the preferential mechanism and existence form, Appl. Catal. A 525 (2016) 76-84.

[17] J.-X. Liu, H.-Y. Su, D.-P. Sun, B.-Y. Zhang, W.-X. Li, Crystallographic dependence of CO activation on cobalt catalysts: HCP versus FCC, J. Am. Chem. Soc. 135 (2013) 16284-16287.

[18] M. Ojeda, R. Nabar, A.U. Nilekar, A. Ishikawa, M. Mavrikakis, E. Iglesia, CO activation pathways and the mechanism of Fischer–Tropsch synthesis, J. Catal. 272 (2010) 287–297.

[19] U. K. Chohan, S. P.K. Koehler, E. Jimenez-Melero, Diffusion of hydrogen into and through ??-iron by density functional theory, Surf. Sci. 672–673 (2018) 56–61.

[20] W. Dong, V. Ledentu, Ph. Sutet, A. Eichler, J. Hafner, Hydrogen adsorption on palladium: a comparative theoretical study of different surfaces, Surf. Sci. 411 (1998) 123-136.

[21] J. Ludwig, D.G. Vlachos, A.C.T. van Duin, W.A. Goddard, III, Dynamics of the dissociation of hydrogen on stepped platinum surfaces using the ReaxFF reactive force field, J. Phys. Chem. B 110 (2006) 4274-4282.

[22] P. Ferrin, S. Kandoi, A. U. Nilekar, M. Mavrikakis, Hydrogen adsorption, absorption and diffusion on and in transition metal surfaces: A DFT study, Surf. Sci. 606 (2012) 679-689.

[23] Q. Wang, R. Zhang, L. Jia, B. Hou, D. Li, Insight into the effect of surface coverage and structure over different Co surfaces on the behaviors of H_2 adsorption and activation, Int. J. Hydrogen Energy 41 (2016) 23022-23032.

[24] P. van Helden, J.-A. van den Berg, C. J. Weststrate, Hydrogen adsorption on Co surfaces: A Density Functional Theory and temperature programmed desorption study, ACS Catal. 2 (2012) 1097-1107.

[25] C.M. Wei, A. Groβ, M. Scheffler, Ab initio calculation of the potential energy surface for the dissociation of H_2 on the sulfur-covered Pd(100) surface, Phys. Rev. B, 57 (1998) 15572-15584.

[26] S. Wilke, M. Scheffler, Poisoning of Pd(100) for the dissociation of H_2: a theoretical study of co-adsorption of hydrogen and sulphur, Surf. Sci. 329 (1995) L605-L610.

[27] E. van Steen, P. van Helden, A DFT study of hydrogen dissociation on CO- and C-precovered Fe(100) surfaces, J. Phys. Chem. C 114 (2010) 5932-5940.

[28] S. Wilke, M. H. Cohen, Influence of potassium adatoms on the dissociative adsorption of hydrogen on Pd (100), Surf. Sci. 380 (1997) L446-L454.

[29] Q. Chen, I.-H. Svenum, Y. Qi, L. Gavrilovic, D. Chen, A. Holmen, E. A. Blekkan, Potassium adsorption behavior on hcp cobalt as model systems for the Fischer–Tropsch synthesis: a density functional theory study, Phys. Chem. Chem. Phys. 19 (2017) 12246-12254.

[30] G. Kresse, J. Hafner, Ab initio molecular-dynamics simulation of the liquid-metal-amorphous-semiconductor transition in germanium, Phys. Rev. B: Condens. Matter Mater. Phys. 49 (1994) 14251-14269.

[31] G. Kresse, J. Furthmüller, Efficiency of ab-initio total energy calculations for metals and semiconductors using a plane-wave basis set, Comput. Mater. Sci. 6 (1996) 15-50.

[32] P.E. Blöchl, Projector augmented-wave method, Phys. Rev. B 50 (1994) 17953-17979.

[33] J.P. Perdew, K. Burke, M. Ernzerhof, Generalized gradient approximation made simple, Phys. Rev. Lett. 77 (1996) 3865-3868.

[34] H.J. Monkhorst, J.D. Pack, Special points for Brillouin-zone integrations, Phys. Rev. B (1976) 5188-5192.

[35] T. Nishizawa, K. Ishida, The Co (cobalt) system, Bull. Alloy Phase Diagrams 4 (1983) 387–390.

[36] G. Henkelman, B.P. Uberuaga, H. Jónsson, A climbing image nudged elastic band method for finding saddle points and minimum energy paths, J. Chem. Phys. 113 (2000) 9901-9904.

[37] G. Henkelman, H. Jónsson. A dimer method for finding saddle points on high dimensional potential surfaces using only first derivatives, J. Chem. Phys. 111 (1999) 7010-7022.

[38] R. van Hardeveld and F. Hartog, The statistics of surface atoms and surface sites on metal crystals, Surf. Sci., 1969, 15, 189-230.

[39] P. van Helden, I.M. Ciobîcã, R.L.J. Coetzer, The size-dependent site composition of FCC cobalt nanocrystals, Catal. Today 261 (2016) 48-59.

[40] G. Connel, J.A. Dumesic, Migration of potassium on iron and alumina surfaces as studied by Auger electron spectroscopy, J. Catal. 92 (1982) 17-24.

[41] H.P. Bonzel, G. Brodén, H.J. Krebs, X-ray photoemission spectroscopy of potassium promoted Fe and Pt surfaces after H_2 reduction and CO/H_2 reaction, Appl. Surf. Sci. 16 (1983) 373-394.

[42] A. Banerjee, V. Navarro, J.W.M. Frenken, A. P. van Bavel, H. P. C. E. Kuipers, M. Saeys, Shape and size of cobalt nanoislands formed spontaneously on cobalt terraces during Fischer−Tropsch Synthesis, J. Phys. Chem. Lett. 7 (2016) 1996-2001.

[43] P. van Helden, J.-A. van den Berg, I. M. Ciobîcã, Hydrogen-assisted CO dissociation on the Co(211) stepped surface, Catal. Sci. Technol. 2 (2012) 491-494.